

TEMPERATURE DISTRIBUTION DURING THE LAMINATION PROCESS OF PV MODULES AND ITS INFLUENCE ON THE DEGREE OF CROSSLINKING FOR EVA - SIMULATION VS. TEST RESULTS

Aksel Kaan Öz, Japan Vasani, Christian Reichel, Christine Wellens, Dirk Holger Neuhaus
Fraunhofer Institute for Solar Energy Systems ISE, Heidenhofstraße 2, 79110 Freiburg, Germany
Corresponding Author: Aksel Kaan Öz | +49 (0) 761 4588 5025 | e-mail: aksel.kaan.oez@ise.fraunhofer.de

ABSTRACT: The lamination process of photovoltaic (PV) modules significantly influences their long-term reliability. One way to control the quality of the lamination process is measuring the degree of crosslinking of the modules, reflecting sufficiency of process parameters like lamination temperature and lamination duration. In this study, we conducted thermocouple measurements across module layers to observe temperature profiles and gauge the degree of crosslinking in glass-backsheet (GB) and glass-glass (GG) modules, both with and without cells. These were compared with the results of a simulation tool that can model the temperature profile and the degree of crosslinking during the lamination. The measurements were compared with the simulations, yielding promising matches with observed values. The simulation effectively captured temperature trends during lamination. Notably, inadequate processing led up to a 6.5% discrepancy in crosslinking between front and back side of modules, a concern addressed by using a plate-plate chamber for GG modules or extending the process duration in the plate-membrane chamber. The study underscored the pronounced influence of cells on crosslinking; their inclusion decreased it by up to 6.5%. Furthermore, we validated the simulation tool's crosslinking prediction against Soxhlet extraction results.

Keywords: PV Modules, Lamination, Degree of Crosslinking, Simulation, Module Manufacturing

1 INTRODUCTION

In recent years, the photovoltaic (PV) industry has witnessed remarkable advancements in cell technologies, sizes, and materials, driven by the pursuit of cost reduction, environmental friendliness, and enhanced module efficiency while ensuring prolonged operational lifetimes with minimal power degradation [1,2]. The lamination process is an important key when it comes to achieving long-term reliability [3]. A robust adhesion among module layers and a good degree of encapsulant crosslinking are essential shields against external stressors, humidity, and other factors that could compromise cell integrity.

To ensure a good lamination process, the optimization of key parameters such as temperature, time, and pressure according to the specific material combinations is essential. Furthermore, it is imperative to achieve a consistent temperature distribution within the module, both laterally but also in the different layers of the module [4].

This paper scrutinizes temperature homogeneity within the module during the lamination process through two distinct methods. Firstly, by comparing the degree of crosslinking in the encapsulant on the front and rear side of the cell, and secondly, by conducting thermocouple measurements to capture the temperature profile within the module during lamination. Additionally, the measurements are compared with simulation from a tool that is capable of modeling the lamination process and is providing temperature data for both the front and rear sides of the cell. The tool may simplify the assessment of new bills of materials (BOM) without the need for time-consuming tests, ultimately leading to valuable time and cost savings.

The study is primarily focused on ethylene-co-vinyl acetate (EVA), the dominant encapsulant in the PV market with approximately 70% market share [5]. To validate our findings, we compare the measured degree of crosslinking and temperature profiles from the lamination process with the simulation results.

In summary, this research sheds light on the critical role of the lamination process in achieving PV module longevity and quality. By investigating temperature homogeneity and introducing a simulation tool, we aim to contribute to streamlined evaluation processes within the PV industry.

2 MATERIALS AND METHODS

In our initial phase, we fabricated six mini modules in both glass-glass (GG) and glass-backsheet (GB) configurations, with three modules for each setup. The modules were laminated with an EVA encapsulant, featuring a size of 680 mm x 370 mm. For both lay-up types (GB, GG) the EVA-GB process was used, which took place in the plate-membrane chamber (HP1) of the Ypsator of Bürkle.

In our extensive study (module matrix shown in Figure 1) we analyzed twelve different conditions and laminated 24 modules. To have a better understanding and reliable results, 2 modules were manufactured for each case and tested twice for their degree of crosslinking. To simplify the sample preparation for the determination of the degree of crosslinking an additional layer of Teflon was introduced between the encapsulant and the glass/rear side layer. Additionally, the lamination process for GB and GG modules was segregated. GB modules underwent lamination in HP1, while GG modules were pre-processed in HP1 and subsequently transferred to the plate-plate chamber (HP2) for crosslinking. The main difference between HP1 and HP2 is that, in HP2 the module is heated actively from both sides and is also in direct contact to the heating plates, whereas in HP1, the module is only in direct contact to the bottom heat plate and gets less heat from the top side.

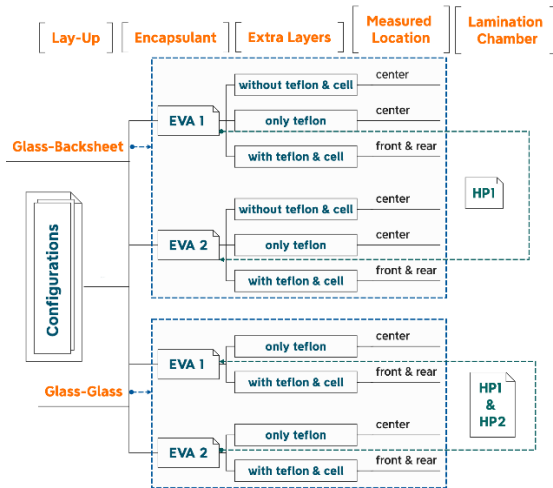


Figure 1: Module Matrix

For the different lay-ups the samples for the Soxhlet extraction were taken from the locations mentioned in Figure 1. The modules including cells were measured on both sides of the cell. The samples of the modules with no solar cells, called “laminates”, were taken from their center. The study also compared the degree of crosslinking of laminates and modules to investigate the influence of cells and also checks for the influence of the Teflon sheet. The specifications of the glasses, encapsulants and other materials used are shown in Table 1.

Table 1: List of used encapsulation materials and their specifications

Layer	Material	Thickness [mm]
glass 1	solar glass	3
glass 2	solar glass	2
backsheet	PET/Primer	0.220
encapsulant 1	EVA	0.500
encapsulant 2	EVA	0.500
teflon sheet	Polytetrafluoroethylene (PTFE)	0.08

2.1 Soxhlet Extraction

To assess the lamination process, the degree of crosslinking values measured on the front and rear side of the PV modules are compared. For this purpose, we adopted Soxhlet extraction, a straightforward time-intensive technique widely used for measuring crosslinking levels in PV modules [6,7].

The Soxhlet degree of crosslinking was calculated by the following formula [6]:

$$X \text{ (Soxhlet)}[\%] = \left(\frac{M_2 - M_0}{M_1 - M_0} \right) \times 100, M_2 \leq M_1$$

where “ M_0 ” indicates the pre-determined weight of the cylindrical stainless steel mesh tube, “ M_1 ” the total weight of the sample in its tube before the process and “ M_2 ” the weight of the sample and its tube after being extracted and dried in the vacuum oven.

The measurements were carried out by using the Behrotest apparatus in accordance with the standard outlined in IEC 62788-1-6. Each module was subjected to at least two sample measurements, the results are presenting the mean value and standard deviation of these measurements.

2.2 Thermocouple Measurements

To precisely monitor the temperature dynamics during lamination, we employed type K thermocouples to measure the actual temperature within a standard-sized module (1960 mm x 1010 mm). Simultaneously, the temperature progression throughout the process was logged using the Datapaq Q18 datalogger. To evaluate the uniformity of heat distribution across the module and comparing the heat variations between its front and rear sides, we strategically positioned four sensors within the module, as depicted in Figure 1.

It is important to note that the PV module lay-up utilized for the thermocouple measurements slightly differs from the standard industry configuration. In our measurement setup, an additional Teflon sheet was inserted between the sensors and the encapsulant. This design modification allows the sensors to be reused for different lay-ups (GB, GG) and distinct processes (EVA-GB, EVA-GG). In Figure 2, the sensors are placed between the inner side of the glass and the additional Teflon sheet, for the GB lay-up, the rear sensors are placed between the backsheet and the Teflon sheet.

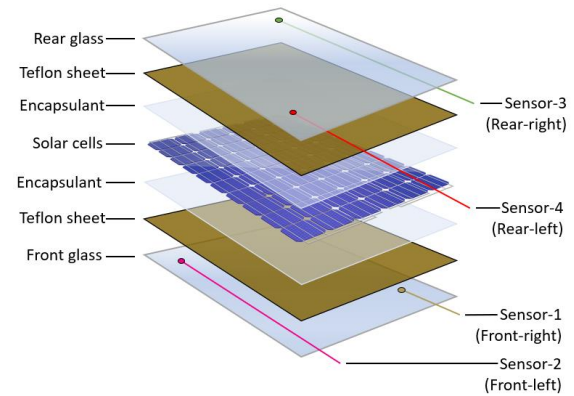


Figure 2: Module lay-up and sensor locations for the thermocouple measurements

2.3 Simulation

The lamination and the crosslinking process of the front and rear EVA in a GB and GG module as shown in Figure 1 is modelled to verify the temperature differences and the experimentally observed degree of crosslinking. A thermal model for photovoltaic modules is developed that determines the one-dimensional temperature distribution within the different module layers, provided by a heating plate in the lamination process [8]. Based on the modelled temperature profile of the EVA in the PV module, a model for the cure kinetics which is used to predict the degree of crosslinking during the lamination process was developed.

In order to achieve the degree of crosslinking of the encapsulation material in the lamination model, the chemical reactions of the EVA is determined by Differential Scanning Calorimetry (DSC), allowing to obtain the crosslinking reaction, which assists in determining the activation energy. The activation energy is calculated using the Friedman kinetic analysis method to see the changes in the degree of crosslinking via the activation energy. To solve the kinetic equation, the kinetic parameters are required with the slope formula to get the activation energy. For the calculation of the kinetic parameters, DSC measurements of the cured sample are taken into account such as reaction that occurs with respect to temperature and time at different heating rates. The activation energy and temperature profile of the encapsulation material are used to acquire the final results for the degree of crosslinking.

The investigated temperature profile is characterized taking into account the material values of the materials used at the module and laminator level. Due to the flexible design of the boundary conditions on both sides of the module, the possibility to extend the module structure (adding or removing any layers from the module) and manufacturing processes (laminators with one heating plate or both side heating plates) is given.

3 RESULTS AND DISCUSSIONS

In this section the degree of crosslinking for the different conditions is analyzed and the results of the simulation are introduced under four main headlines. These are the comparison of the degree of crosslinking on the front and rear side of the cell, the change in degree of crosslinking after including cells into the laminate, the temperature profile during lamination versus the simulation and the degree of crosslinking curve, respectively.

3.1 Front versus Rear Crosslinking

In the initial trial, all laminates and modules underwent the EVA 1 GB process in the plate-membrane chamber. In the extensive study, we employed different EVAs and alternated between the GB process and GG process based on module lay-up. The results obtained are shown in Figure 3.

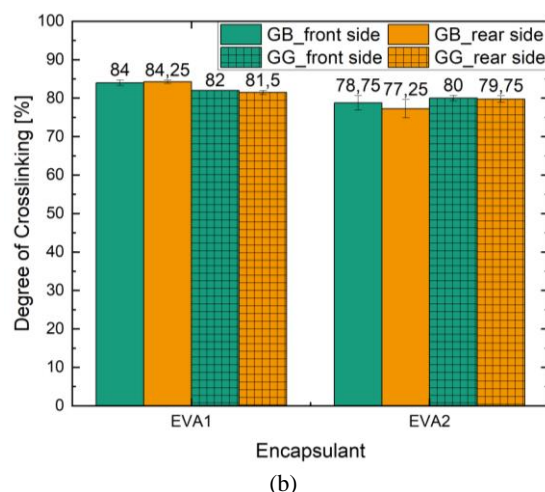
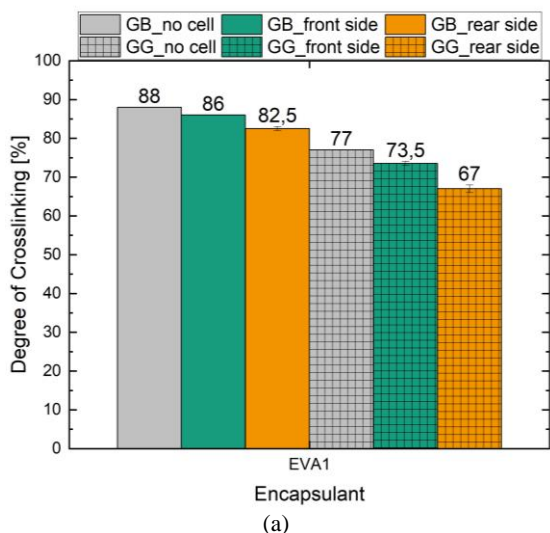


Figure 3: Comparison of the degree of crosslinking on the front/rear side of the module, (a) for initial trial, (b) for extensive study

The results, illustrated in Figure 3 (a), highlight a noteworthy reduction in crosslinking for all GG modules in the initial trial. This decrease, particularly evident in the 6.5% difference between rear and front side crosslinking in the GG module, suggests a temperature disparity between both sides. This difference is attributed to the lamination process occurring primarily in the GB process. For improved temperature transmission and crosslinking uniformity in GG modules, an extended process duration in HP1 or transitioning to HP2 (plate-plate chamber) for GG modules is recommended (Figure 6).

In Figure 3 (b), a reduced difference in crosslinking between front vs. rear side is observed compared to Figure 3 (a). This improvement is attributed to GG modules being laminated in a combination of HP1 and HP2, facilitating better temperature transmission and crosslinking uniformity. Notably, EVA2 consistently exhibited lower crosslinking compared to EVA1. A potential reason might be differences in the amount of curing agents in the encapsulant or that the used process was more suitable for EVA1 [9].

3.2 Laminate versus Module Crosslinking

Given the lower crosslinking degrees observed for modules (with cells) compared to laminates (without cells) in the initial trial, we examined the influence of cells on crosslinking. While laminates were sampled from the center, module sampling was constrained by solar cells. The degree of crosslinking of the GB module and GG module in Figure 4 shows the mean values measured on the front and rear side of the modules.

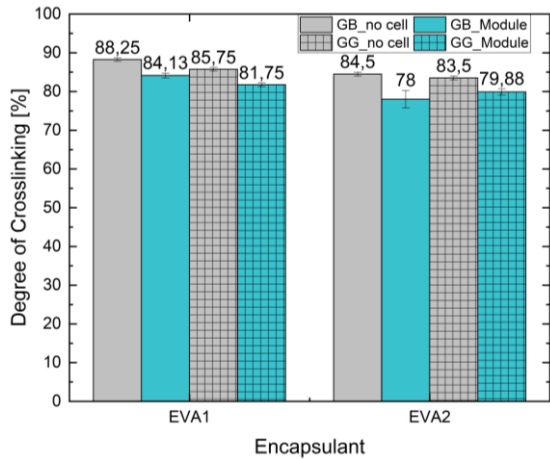


Figure 4: Influence of solar cells on the degree of crosslinking

Figure 4 presents the crosslinking degrees for the GB and GG modules, revealing differences ranging from 3.5% to 6.5%, based on module lay-up and encapsulant. The graph highlights a reduction in crosslinking after inserting cells for all cases. Notably, the difference remained relatively stable (around 4%) with EVA1, while EVA2 was more influenced by the lay-up.

3.3 Temperature Profile during Lamination

To investigate the crosslinking disparities between the front and rear side of the module, we studied the temperature profile during lamination. The exact locations of the sensors are shown in Figure 2. The results of the thermocouple measurements and the simulations for the GB and GG processes together with their lamination parameters are compared in and Figure 6.

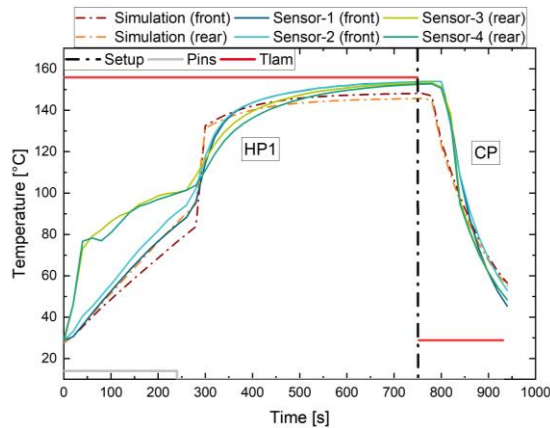


Figure 5: Temperature profile during the lamination process for a glass-backsheet module and lamination process parameters of the glass-backsheet process used in this study

The simulated temperature process follows the thermocouple measurements, demonstrating consistency in temperature evolution. In both a certain temperature raises out to 240 seconds is observed, after this point, both show initially a faster increase in temperature followed by a smoother curve. At this point the pins go down and the module gets in direct contact with the heating plate, which provides a faster temperature transfer.

After 750 seconds the module goes from HP1 to the cooling press CP where it is cooled down. In the

measurement we can see a small delay compared to the simulation, because in reality it takes some seconds while the module is transferred from one chamber to the other.

The results indicate that the length of the process is almost optimal. The maximum temperatures reached by the sensors on the front and rear side are 153.9 °C and 153.4 °C, respectively. For the simulation these values are 148.2 °C and 145.7 °C whereas the set temperature off the process was 155 °C.

An interesting observation was the temperature profile at the beginning of the process, where the rear side of the module had a higher temperature compared to the front side. This phenomenon was also observed in the simulation. The reason for that might be, that at that point there is no direct contact on both sides, the module lies on the pins and the heat transfer through the backsheet is going faster compared to the glass on the front side. However, for a reliable statement further research needs to be done.

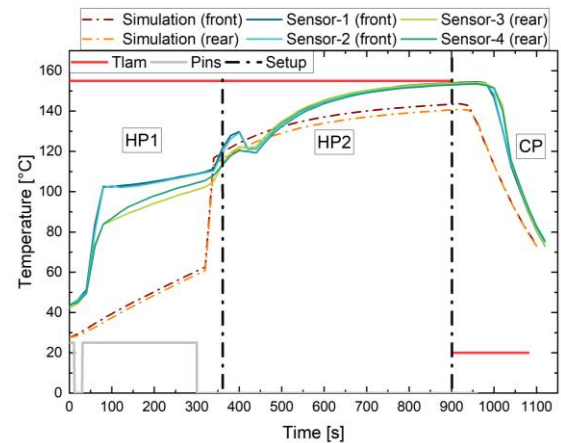


Figure 6: Temperature profile during the lamination process for a glass-glass module and lamination process parameters of the glass-glass process used in this study

Figure 6 shows that our simulation tool also simulated promising results in comparison to the outcomes of the measurements. This time the measurements show a higher temperature on the front side of the module compared the rear side, different as observed in the GB module lay-up. There are two main reasons for this. One is the short direct contact (when the pins are down) at the beginning of the process. The other factor is that this time we have a GG module with same thermal characteristics on both sides.

Same as in , the influence of the pins and the delay in cooling while the transfer to the CP can be easily read from Figure 6. In addition to these, the GG module is also going through the phase where it enters the HP2, here it is heated actively from both sides. That provides a better heat transfer and helps that a homogeneous temperature is reached on both sides of the module. In this phase the temperature gap from HP1 closes and the temperature on both sides approaches each other.

The first thing that attracts the attention when comparing the simulation and the measurement is the temperature profile in the first 300 seconds. In the GG process shown in Figure 6 the pins are going down at the beginning and then go up again. This causes a direct contact with the heating plate, resulting in a fast temperature transfer. However, after the pins go up again, the temperature curve becomes flatter. The influence of this small step was not considered and therefore neglected in the simulation. This might also be the explanation for the

difference in peak temperatures. The peak temperatures on the front and rear side measured are 154.4 °C and 154.1 °C, in the simulation, however, these are 143.6 °C and 140 °C, respectively.

Another point is the measured decrease in temperature between 350 and 400 seconds. Here the module is transferred from HP1 to HP2. The contact with the room temperature during this time is causing this small decrease. In the simulation this was not considered.

3.4 Degree of Crosslinking Curve

Our simulation tool also enables crosslinking degree predictions, potentially avoiding the need for costly and time-consuming prototype production and testing.

The results of the simulation are compared with the measurements conducted in our previous study, where we analyzed the degree of crosslinking over time for different curing durations at 150° C (see Figure 7) [2]. The simulation parameters were adopted. The glass thickness was changed to 3.2 mm and the lamination temperature was set to 150 °C, instead of 155 °C.

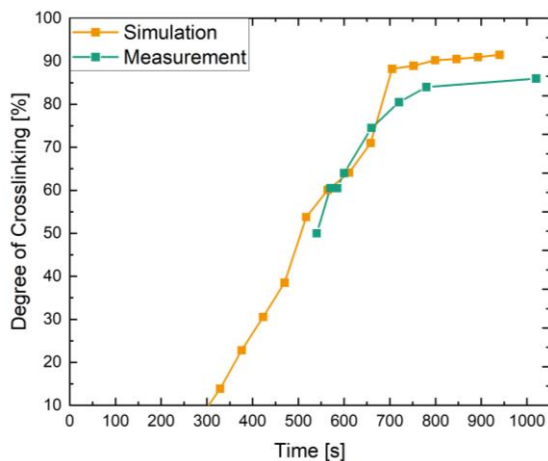


Figure 7: Simulated and measured degree of crosslinking over time for an EVA1, glass-backsheet module

Comparing simulation results with measurements from our prior study (Figure 7), we observed good agreement for most of the process. However, a divergence emerges after the 660 seconds, reaching a 5% difference at the end of the process (91% simulation versus 86% measurement). Therefore, we are investigating improvements on the simulation tool.

In summary, the results emphasize the significance of module lay-up, encapsulant choice, and temperature profiles in determining crosslinking uniformity and stability in photovoltaic modules.

4 CONCLUSION AND OUTLOOK

In conclusion, this study reveals crucial aspects of the lamination process for photovoltaic modules and its impact on crosslinking behavior. Through a systematic analysis of various module lay-ups, encapsulant materials, and process parameters, several significant findings have emerged.

Firstly, our initial investigation into the comparison of crosslinking on the front and rear sides of the module revealed that the degree of crosslinking was 6.5% lower on the rear side of glass-glass (GG) modules compared to the front side, indicating a temperature difference between

the sides. This difference is attributed to the lower temperature transfer at the plate-membrane chamber or the lamination duration. To mitigate this, active heating on both sides during lamination, or extending the process duration in HP1 is proposed. Notably, the encapsulant type significantly influenced the crosslinking outcome, with EVA2 consistently exhibiting lower degrees of crosslinking compared to EVA1 when processed at the same temperature.

Moreover, incorporating cells into the laminate led to an important observation, the degree of crosslinking decreased by 3.5% to 6.5%. This shows the influence of cells on the degree of crosslinking and that this factor should not be neglected.

The temperature profile during lamination, analyzed through thermocouple measurements and simulation, exhibited a high degree of conformity between the two methods. Notably, the simulated temperature peaks closely matched the measured values, reaching 148.2 °C on the front and 145.7 °C on the rear side for GB modules. Additionally, the degree of crosslinking curve, simulated to save time and resources, exhibited a commendable alignment with measurements. Although a slight discrepancy was noted after 660 seconds, the simulation maintained a satisfactory correspondence, underscoring its practical value.

These results collectively illuminate key factors influencing the lamination process and crosslinking behavior in photovoltaic modules. Our findings not only contribute to enhancing the understanding of module manufacturing but also offer a validated simulation tool for predicting crosslinking behavior. With implications for module quality, reliability, and operational stability, this study provides valuable insights that could help to improve manufacturing processes.

In prospect, further research can delve deeper into optimizing process parameters, exploring advanced encapsulant materials, and extending the applicability of the simulation tool to various scenarios.

5 ACKNOWLEDGEMENT

This work was supported by the German Federal Ministry for Economic Affairs and Energy (BMWi) under the contract number 0324287C, acronym GEPARD.

6 REFERENCES

- [1] Cattaneo, Gianluca & Faes, Antonin & Li, Heng-Yu & Galliano, Federico & Gragert, Maria & Yao, Yu & Grischke, Rainer & Söderström, Thomas & Despeisse, Matthieu & Ballif, Christophe & Perret-Aebi, Laure-Emmanuelle, Lamination process and encapsulation materials for glass-glass PV module design, *Photovoltaics International* (2015).
- [2] A.K. Öz, C. Wellens, M. Mittag, M. Wiese, S. Sraith, D. Klaus et al., 2.5 Minutes Lamination Process and the Influences of the Degree of Cross-Linking and the Moisture Ingress on the Degradation of PV Modules, 7 pages / 8th World Conference on Photovoltaic Energy Conversion; 816-822 (2022).
- [3] A.K. Öz, C. Herzog, C. Wellens, D.E. Mansour, M. Heinrich, A. Kraft, The Impact of the Lamination Process on the Adhesion Properties at the Glass-Encapsulant Interface and Damp Heat Stability of PV Modules, 7 pages / 38th European Photovoltaic

- Solar Energy Conference and Exhibition; 708-714 (2021).
- [4] S. Sraisth, A.K. Öz, D. Klaus, C. Wellens, M. Heinrich, Influence of the Lamination Pressure on the Adhesion, Degree of Cross-Linking, and Bubble Formation of PV Modules, 7 pages / 8th World Conference on Photovoltaic Energy Conversion; 823-829 (2022).
- [5] M. Fischer, M. Woodhouse, P. Baliozian, J. Trube, International Technology Roadmap for Photovoltaic (ITRPV) 14 (2023).
- [6] C. Hirschl, L. Neumaier, S. Puchberger, W. Mühleisen, G. Oreski, G.C. Eder et al., Determination of the degree of ethylene vinyl acetate crosslinking via Soxhlet extraction: Gold standard or pitfall?, *Solar Energy Materials and Solar Cells* 143 (2015) 494–502.
- [7] C. Lux, U. Blieske, E. Malguth, N. Bogdanski, Variations in Cross-Link Properties of EVA of Un-Aged and Aged PV-Modules, 5 pages / 29th European Photovoltaic Solar Energy Conference and Exhibition; 2462-2466 / 29th European Photovoltaic Solar Energy Conference and Exhibition; 2462-2466 (2014).
- [8] M. Mittag, L. Vogt, C. Herzog, A. Pfreundt, J. Shahid, D.H. Neuhaus et al., Thermal Modelling of Photovoltaic Modules in Operation and Production, 9 pages / 36th European Photovoltaic Solar Energy Conference and Exhibition; 892-900 (2019).
- [9] G.M. Wallner, B. Adothu, R. Pugstaller, F.R. Costa, S. Mallick, Comparison of Crosslinking Kinetics of UV-Transparent Ethylene-Vinyl Acetate Copolymer and Polyolefin Elastomer Encapsulants, *Polymers* 14 (2022).